

Ultrafast Exciton Dynamics in CdSe Quantum Dots Studied from Bleaching Recovery and Fluorescence Transients

Haiyu Wang,[‡] Celso de Mello Donegá,[§] Andries Meijerink,[§] and Max Glasbeek^{*,‡}

Laboratory for Physical Chemistry, University of Amsterdam, Nieuwe Achtergracht 129, 1018 WS Amsterdam, The Netherlands, and Condensed Matter and Interfaces, Debye Institute, Utrecht University, P.O. Box 80000, 3508 TA Utrecht, The Netherlands

Received: October 11, 2005; In Final Form: November 22, 2005

We have performed ultrafast absorption bleach recovery and fluorescence upconversion measurements (~ 100 fs time resolution) for three CdSe samples, with nanoparticle diameters of 2.7, 2.9, and 4.3 nm. The two types of experiments provide complementary information regarding the contributions of the different processes involved in the fast relaxation of electrons and holes in the CdSe quantum dots. Transient absorption and emission experiments were conducted for the $1S$ [$1S(e) - 1S_{3/2}(h)$] transition, $1S(e)$ and $1S_{3/2}(h)$ representing the lowest electron (e) and hole (h) levels. The bleach recovery of the $1S$ transition shows a ~ 400 – 500 fs initial rise, which is followed by a size-dependent ~ 10 – 90 ps decay and finally a long-lived (\sim ns) decay. The fluorescence upconversion signal for the $1S$ transition shows quite different temporal behavior: a two times slower rise time (~ 700 – 1000 fs) and, when the fluorescence upconversion signal has risen to about 20% of its maximum intensity, the signal displays a slight leveling off (bend), followed by a continued rise until the maximum intensity is reached. This bend is well reproducible and power and concentration independent. Simulations show that the bend in the rise is caused by a very fast decay component with a typical time of about 230–430 fs. Considering that the $1S$ quantum dot excitation is comprised of five exciton substates ($F = \pm 2, \pm 1^L, 0^L, \pm 1^U$, and 0^U), we attribute the disparity in the rise of the bleaching and emission transients to the results from the dynamics of the different excitons involved in respectively the bleaching and fluorescence experiments. More specifically, in transient absorption, population changes of the $F = \pm 1^U$ excitons are probed, in emission population effects for the $F = \pm 2$ (“dark”) and the $F = \pm 1^L$ (“bright”) exciton states are monitored. It is discussed that the fast (~ 400 – 500 fs) rise of the bleach recovery is representative of the feeding of the $F = \pm 1^U$ exciton (by filling of the $1S(e)$ electron level) and that the slower (~ 700 – 1000 fs) feeding of the emissive $\pm 2, \pm 1^L$ excitons is determined by the relaxation of the hole levels within the $1S_{3/2}$ fine structure. Finally, the ~ 230 – 430 fs component, typical of the bend in the fluorescence transient, is attributed to the thermalization of the close-lying ± 2 (“dark”) and $\pm 1^L$ (“bright”) excitons.

Introduction

Semiconducting nanocrystals (NC's) exhibit interesting optical and electronic properties due to quantum confinement.^{1,2} Numerous investigations have focused on the dynamics of charge carriers in semiconductor nanoparticles.^{3–12} In these studies, the very rapid (subpico-to-picosecond) relaxation of electrons has attracted much attention.^{6–12} The electron relaxation is orders of magnitude faster than expected when only electron–phonon interactions are considered. Electron relaxation is fast because of Auger-type relaxation, i.e., electron–hole coupling efficiently transfers excess electron energy to holes that relax extremely fast because of their high-density band-like structure.¹³

Many relaxation experiments concern quantum dot samples of CdSe. Bleaching recovery experiments, performed for monodisperse colloidal NC's, revealed electron relaxation times of ~ 300 fs.^{6–8} Moreover, from time-resolved photoluminescence studies of the band gap emission also a relatively slow component in the relaxation of holes, as slow as ~ 700 fs, could

be resolved.¹⁴ The “slow” component was attributed to a multiphonon relaxation process involving discretely dispersed hole levels near the bottom edge of the valence band.

In this paper, we perform a comparative study of bleaching recovery and emission transients measured for three CdSe samples, containing nanoparticles with diameter sizes of 2.7, 2.9, and 4.3 nm, respectively. The transient absorption and emission experiments were performed for the $1S$ [$1S(e) - 1S_{3/2}(h)$] transition, where $1S(e)$ and $1S_{3/2}(h)$ represent the lowest electron (e) and hole (h) levels in the usual notation.¹⁵ Since this transition is nominally the same in absorption and emission, at first sight, it might seem that the same temporal behavior is expected in the two experiments. However, in comparing the kinetics of the bleaching and emission transients, it is of great importance to take into account the fine structure splittings of the $1S_{3/2}(h) - 1S(e)$ exciton. This exciton is 8-fold degenerate for spherically symmetric dots, but, due to electron–hole exchange interactions, the crystal field of a hexagonal lattice, and crystal shape asymmetry, the degeneracy is lifted (Figure 1). The exciton is split into five states: $F = \pm 2, \pm 1^L, 0^L, \pm 1^U$, and 0^U , F being the total exciton angular momentum projection given by the sum of the electron ($1/2$) and hole ($3/2$) spin

* Address correspondence to this author. E-mail: glasbeek@science.uva.nl

[‡] University of Amsterdam.

[§] Utrecht University.

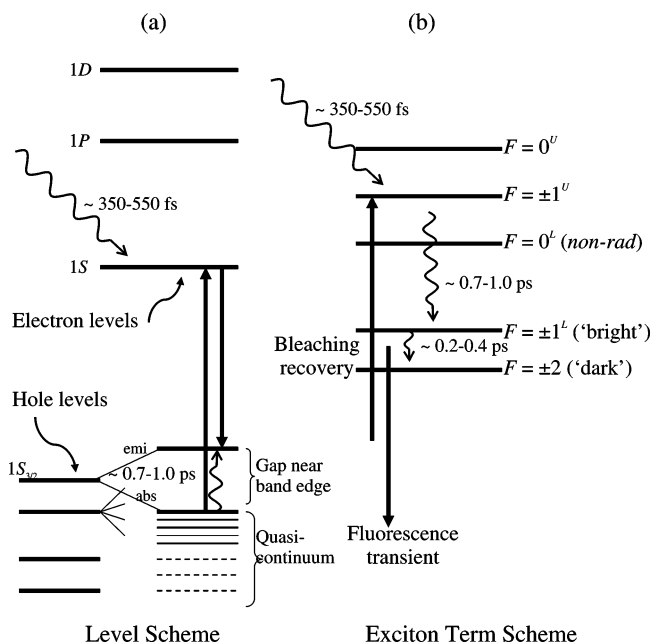


Figure 1. (a) Scheme of lowest electron and hole level energies in CdSe quantum dot. Splittings include the effects of crystal field, nonspherical shape, and spin-orbit couplings; the influence of e-h exchange interactions has not yet been taken into account. Note the discreteness of the levels of the “emissive” and “absorptive” $1S_{3/2}$ holes near the band edge. (b) Term scheme for exciton states involved in $1S_{3/2}(h) - 1S(e)$ excitation which, in addition to the single particle energies of part a, also includes the effects of e-h exchange interactions. The bleach recovery experiment measures the restoration of the population of the $F = \pm 1^U$ excitons by filling of the $1S$ electron levels, the filling of the “absorptive” hole level from the “quasi”-continuum being too fast to be measured; the fluorescence upconversion experiment measures the feeding and decay of the $F = \pm 2$ and $\pm 1^L$ (“dark” and “bright”) exciton states.

projections.^{16,17} Of these split states, the exciton ground state is the $F = \pm 2$ state, with an energy only a few millielectronvolts (~ 0.13 meV for the bulk, ~ 13 meV for 2 nm dots)¹⁷ below that of the $F = \pm 1^L$ state. The oscillator strengths of the different fine structure states are not equal and this is why different transitions are involved in absorption and emission. Within the electric dipole approximation direct excitation of the $F = \pm 2$ and 0^L excitons is optically forbidden, while the $\pm 1^U$ excitons have a larger oscillator strength than the $\pm 1^L$ excitons.^{4,17} In linear absorption, the first band corresponds to the excitation of the $F = \pm 1^U$ excitons. In emission, although formally the $F = \pm 2$ exciton ground state is optically inactive (hence the labeling “dark” state), the transition from this state becomes weakly allowed by relaxing the selection rules through mixing of the closely spaced levels. The intrinsic radiative lifetime of the $F = \pm 2$ state is about $1 \mu\text{s}$.¹⁸ At room temperature, thermalization with the optically active $F = \pm 1^L$ (“bright”) exciton state is rapid and steady-state emission is due to the ± 2 as well as the $\pm 1^L$ excitons.^{3,4}

The discrete splitting of the $1S_{3/2}$ hole levels (Figure 1a), imposed by the hexagonal internal crystal field, the nonspherical dot shape, and spin-orbit coupling, is of great relevance in comparing the optical transitions involved in emission and absorption. The $1S_{3/2}(h) - 1S(e)$ exciton emission involves the energetically lowest $1S_{3/2}$ fine structure levels (represented by the upper hole-level lines, the “emitting” hole levels, in Figure 1a) only. On the other hand, in the transient absorption experiment, recovery of the $F = \pm 1^U$ excitons is measured; these excitons also involve the $1S_{3/2}(h) - 1S(e)$ transition, but now only the energetically higher lying hole levels of the $1S_{3/2}$

manifold contribute. The latter (the “absorbing” hole levels of Figure 1a) are embedded in a high-density band, characteristic of highly excited holes, so that in the transient absorption experiment, they become almost instantaneously (< 100 fs) refilled. Figure 1a gives a qualitative scheme of the lower electron and hole level energies without consideration of the effects of e-h exchange interaction (single-particle model); Figure 1b gives a qualitative picture of the term scheme comprising the energies of the exciton states resulting from the $1S_{3/2}(h) - 1S(e)$ excitation when e-h exchange interaction has been taken into account. The dynamics displayed by the bleaching and emission transients of the CdSe NC's could be different because different transitions are probed: bleaching recovery involves the population dynamics of the $F = \pm 1^U$ exciton state, whereas the emission transients are representative of the dynamics of the, nominally optically forbidden, $F = \pm 2$ (“dark”) exciton and the optically active $F = \pm 1^L$ (“bright”) exciton states.¹⁴ Here, we demonstrate a disparity in the rise dynamics for the bleach recovery and fluorescence upconversion transients for the same CdSe sample. The disparity is explained by considering that the bleach is determined by fast filling of the $1S(e)$ electron level, whereas the fluorescence rise is attributed to slowed relaxation within the “absorbing” and “emitting” $1S_{3/2}$ fine structure hole levels. Furthermore, the detection of the fluorescence rise allows us to temporally resolve the “bright”-to-“dark” exciton relaxation. The characteristic time for this process is found to be ~ 230 – 430 fs, depending on the size of the NC's.

Experimental Section

The nanocrystal CdSe samples were prepared by a hot injection method described in detail in ref 19. As demonstrated,¹⁹ choosing suitable growth conditions (Cd:Se ratio of 1:5, growth temperature of 240°C , surface passivation in a TOPO:HDA:TOP coordinating solvent, where TOPO = trioctylphosphine oxide, HDA = hexadecylamine, and TOP = trioctylphosphine), highly luminescent (quantum yield: $\sim 90\%$), nearly monodisperse CdSe nanocrystals are reproducibly obtained, making a postpreparative treatment (as for example overcoating with ZnS) unnecessary. In addition, the prepared NC's show the advantage of defect-free and well-passivated surfaces. The NC's were suspended in chloroform in a concentration of about 10^{-5} M.

Steady-state absorption spectra were recorded by means of a conventional spectrophotometer (Shimadzu, UV-240). Steady-state fluorescence spectra were measured with the emission spectrometer described before.²⁰ In these experiments excitation was at 323 nm; the emission spectra were corrected for the wavelength-dependent sensitivity of the monochromator-photomultiplier detection system. All experiments were performed at room temperature.

Femtosecond fluorescence upconversion transients were measured by means of the setup described previously.²¹ The system response time, as measured from the cross-correlation signal of the excitation and gating pulses at 360 and 800 nm, was estimated to be approximately 280 fs (fwhm). The measured transients were fitted to multiexponential functions convoluted with the system response function. The experimental time resolution (after deconvolution) was approximately 100 fs. In the upconversion experiments, the excitation wavelength was at 360 nm, and the transients were detected from 500 nm up to 620 nm. To remove contributions from rotational reorientation motions of the solute molecules, measurements were performed under magic angle conditions (with the laser-excitation polarization at an angle of 54.7° relative to the vertically polarized gating

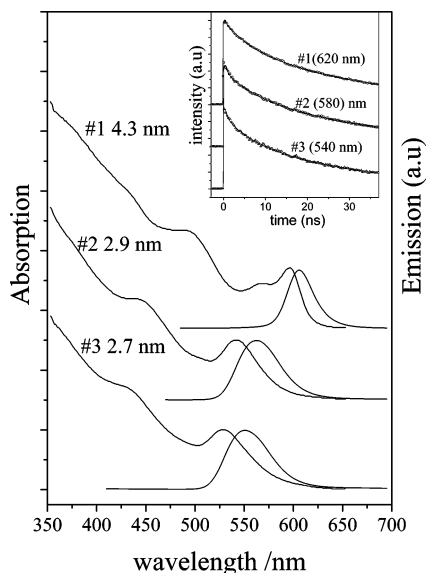


Figure 2. Steady-state absorption and emission spectra of CdSe nanocrystals, with sizes of 2.7, 2.9, and 4.3 nm. The insert shows band-edge fluorescence kinetics measured by means of TCSPC setup at the detection wavelengths given in parentheses.

beam). For time windows longer than 150 ps, the fluorescence transients were detected by using the time-correlated single-photon-counting (TCSPC) setup described previously.²⁰ In these experiments the wavelength of the laser pulses was kept at 323 nm; the instrument response was about 16 ps (fwhm).

In the femtosecond transient absorption experiments, the pump (at 360 nm) is generated by the laser system (Hurricane (Spectra-Physics), 800 nm pulse, 120 fs pulse duration, and OPA-800 C), while the probe is a white light continuum pulse generated by focusing the 800 nm beam into a sapphire plate. The detector is a 2048-pixels CCD camera (Ocean Optics, S2000). The experimental time resolution (after deconvolution) was approximately 100 fs.

Results

Steady-State Absorption and Emission. Absorption and emission spectra of CdSe nanocrystals with sizes of 2.7, 2.9, and 4.3 nm, are given in Figure 2. The absorption spectra show structural features typical of interband optical transitions coupling different quantized electron and hole states.¹⁵

Two absorption bands, at 595 (2.08 eV) and 570 nm (2.17 eV), are resolved for the 4.3 nm sample. These bands are assigned as 1S [$1S(e) - 1S_{3/2}(h)$] and 2S [$1S(e) - 2S_{3/2}(h)$] transitions,⁷ where 1S(e), $1S_{3/2}(h)$, and $2S_{3/2}(h)$ represent the lowest electron (e) and hole (h) levels in the usual notation.¹⁵ For the smaller sized NC's, the 1S and 2S bands are blue shifted; furthermore, because of increased inhomogeneous broadening, these two bands can no longer be separately resolved. The steady-state emission spectrum (excitation at 323 nm) is dominated by the band-edge emission. The size-dependent Stokes shift varies from 80 to 100 meV; the shift is due to the combined effects of confinement-enhanced e–h exchange energy, internal crystal fields, and shape anisotropy.¹⁷ Our samples do not show the deep trap emission (~ 885 nm) that has been attributed to electron/hole recombination to surface states.¹²

Time-Resolved Absorption and Fluorescence Transients. Applying pump pulses at 360 nm, we performed time-resolved measurements of the bleaching of the absorption bands of CdSe quantum dots ($d = 2.7, 2.9, 4.3$ nm) at wavelengths from 500

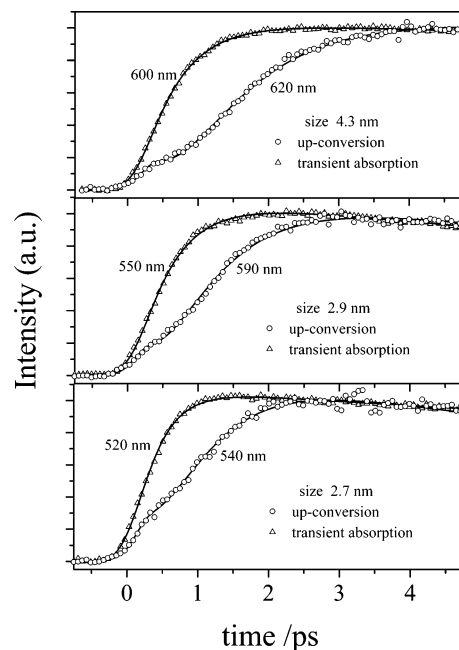


Figure 3. Fluorescence upconversion and absorption transients of CdSe nanocrystals with sizes of 2.7, 2.9, and 4.3 nm.

TABLE 1: Best-Fit Parameters of Deconvoluted Absorption Bleach Transients to the Function $I \propto \sum_i A_i \exp(-t/\tau_i)^a$

	transient absorption/nm	τ_1 /ps	τ_2 /ps	τ
4.3 nm	570	0.58 (–1)	84 (0.6)	\sim ns (0.4)
	600	0.53 (–1)	90 (0.6)	\sim ns (0.4)
2.9 nm	520	0.50 (–1)	9.8 (0.9)	\sim ns (0.1)
	550	0.53 (–1)	24 (0.7)	\sim ns (0.3)
2.7 nm	570	0.54 (–1)	46 (0.6)	\sim ns (0.4)
	500	0.40 (–1)	7.9 (0.5)	\sim ns (0.5)
	520	0.35 (–1)	14 (0.4)	\sim ns (0.6)
	550	0.39 (–1)	10 (0.5)	\sim ns (0.5)

^a Relative weights (A_i) are given in parentheses.

to 600 nm (Figure 3). The bleaching transients could be fitted to multiexponential functions convoluted with the system response function; the parameter values for the best-fit curves are listed in Table 1. The accuracy of the subpicosecond absorption bleach time constants (τ_1) given in Table 1 is better than 5%. The transients show an initial rise with a characteristic time of 400–500 fs, followed by a size-dependent decay (~ 10 ps for $d = 2.7$ nm, ~ 90 ps for $d = 4.3$ nm) and finally a long-lived (\sim ns) decay. The subpicosecond rise of the bleach of the CdSe NC's is in agreement with previous reports.^{6–8} The ~ 500 fs rise of the bleach has been attributed to the filling of the lowest electron states. Hole-state filling processes (involving changes of small occupation numbers over many adjacent levels) are much faster and their contribution to the bleach recovery dynamics is negligible.^{5,9,22}

The lifetime of the band-edge emission was measured utilizing the time-correlated single-photon counting setup (time resolution ~ 16 ps).²⁰ The fluorescence decays for all NC samples (excitation pulses at 323 nm) have a multiexponential form because of quantum dot inhomogeneities (size, surface, shape). Typical lifetimes vary from several hundreds of picoseconds, several nanoseconds, to several tens of nanoseconds, depending on quantum dot size and emission wavelength (Table 2). The long lifetimes are in support of the mediation of long-lived “dark” exciton states in the band-edge emission. In particular, thermal equilibrium between the radiative $F = \pm 1^L$ and nonradiative $F = \pm 2$ states will result in a relatively long

TABLE 2: Best-Fit Parameters of TCSPC Fluorescence Transients with the Function $I \propto \sum_i A_i \exp(-t/\tau_i)^a$

	fluorescence transient/nm	τ_1 /ps	τ_2 /ns	τ_3 /ns
4.3 nm	570	375 (0.28)	4.6 (0.28)	24.1 (0.44)
	610	497 (0.20)	5.5 (0.30)	27.6 (0.50)
	620	263 (0.18)	6.2 (0.23)	32.4 (0.59)
	650	315 (0.20)	5.9 (0.14)	41.6 (0.66)
2.9 nm	540	312 (0.29)	5.6 (0.22)	25.2 (0.49)
	560	379 (0.25)	6.7 (0.23)	30.6 (0.52)
	580	410 (0.25)	6.4 (0.16)	33.1 (0.59)
2.7 nm	540	419 (0.26)	5.6 (0.22)	26.5 (0.51)
	570	388 (0.25)	5.4 (0.21)	30.6 (0.53)

^a Relative weights (A_i) are given in parentheses.

TABLE 3: Best-Fit Parameters of Femtosecond Fluorescence Upconversion Transients with the Function $I \propto \sum_i A_i \exp(-t/\tau_i)^a$

	fluorescence transient/nm	τ_1 /ps	τ_2 /ps	τ_3 /ps	τ_4
4.3 nm	500	0.99 (-0.8)	0.29 (0.34)	9.0 (0.63)	~ns (0.03)
	520	0.99 (-0.8)	0.23 (0.33)	10.0 (0.58)	~ns (0.09)
	550	0.98 (-0.8)	0.41 (0.43)	13.6 (0.42)	~ns (0.15)
	580	1.08 (-1)	0.35 (0.41)	54 (0.44)	~ns (0.15)
	620	0.96 (-0.9)	0.43 (0.58)	84 (0.42)	~ns (0.13)
	600	0.84 (-0.9)	0.33 (0.50)	11.1 (0.40)	~ns (0.10)
2.9 nm	550	0.81 (-0.8)	0.35 (0.51)	15.2 (0.32)	~ns (0.17)
	570	0.87 (-0.9)	0.30 (0.47)	17.0 (0.40)	~ns (0.13)
	600	0.84 (-0.9)	0.33 (0.50)	11.1 (0.40)	~ns (0.10)
2.7 nm	510	0.85 (-0.9)	0.30 (0.41)	11.2 (0.42)	~ns (0.17)
	540	0.85 (-0.9)	0.31 (0.45)	12.2 (0.38)	~ns (0.17)
	570	0.71 (-0.9)	0.31 (0.51)	11.5 (0.38)	~ns (0.11)
	600	0.70 (-0.9)	0.30 (0.45)	8.8 (0.42)	~ns (0.13)

^a Relative weights (A_i) are given in parentheses.

lifetime. Since the size of the quantum dot will sensitively affect the energetic spacing of these radiative and nonradiative excitons, the inhomogeneity in the quantum dot size will result in a spread in the fluorescence decay times and hence a nonexponential (detection wavelength dependent) fluorescence decay.

Figure 3 includes the initial part of the fluorescence upconversion transients detected for the band-edge emission of the three CdSe samples, with $d = 2.7, 2.9,$ and 4.3 nm particles. Of interest is the comparison of the temporal behavior of the emission and bleaching transients measured for the same CdSe samples. Clearly, different rise rates are observed for the emission and bleach transients of the same sample, the build-up of the former being appreciably slower. Fits to convoluted multiexponential functions (drawn lines) showed that the rise times are approximately 700–1000 fs, i.e., about two times those for transient bleaching (Table 3). Furthermore, when the upconversion signal has reached about 20% of its maximum intensity at ~ 500 fs, a bend in the signal is observed that is well reproducible and power and concentration independent (Figure 4). Simulations show that the bend is caused by a slight very fast decay component with a typical time of about 230–430 fs (τ_2 in Table 3; the accuracy of the τ_2 values is approximately 10%). The bend is followed by a ~ 700 – 1000 fs rise until after about 2–3 ps the signals show a decay with a time of about several picoseconds to several tens of picoseconds (τ_3) and a long-lived tail, depending on quantum dot size and emission wavelength (Table 3). In contrast to the excitation power independence of the subpicosecond components (rise and bend), the 10–20 picosecond decay component, τ_3 , turned out to be strongly power dependent (inset in Figure 4).

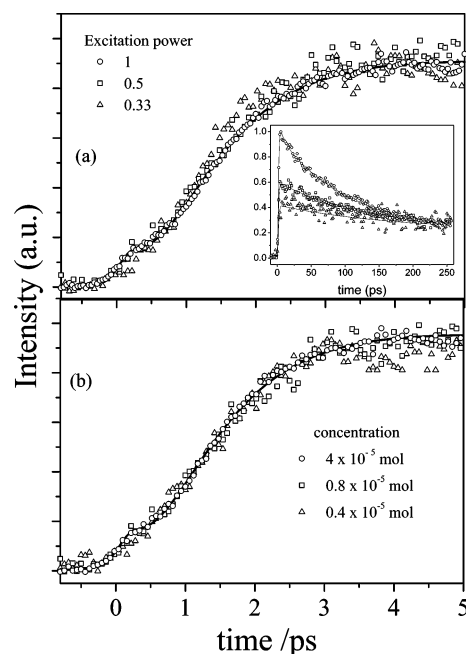


Figure 4. Femtosecond fluorescence upconversion transients of CdSe nanocrystals for various laser pump powers (a) and for various concentrations (b). The inset shows transients for long time windows.

Discussion

The 350–550 fs rise of the bleach signals (Table 1, Figure 3) is in agreement with previous reports.^{6–8} The rise of the bleaching is attributed to filling of the lowest $1S(e)$ electron level by intraband $1P \rightarrow 1S$ electron relaxation, after pumping the $1P$ and $1D$ levels. Rapid intraband electron relaxation has been explained assuming Auger-type energy transfer from electrons to holes, that relax extremely fast (faster than the time resolution of ~ 100 fs of our experiments) because of the dense spectrum of hole levels.^{11,13,23} Recently, subpicosecond Auger times for CdSe colloidal quantum dots were also calculated from theory.²³ Electron filling thus determines the bleach recovery which, as pointed out in the Introduction, in fact corresponds to the build-up of $F = \pm 1^U$ quantum dot excitons. Note from Table 1 that for the smaller sized quantum dots the τ_1 values are shorter, implying a somewhat faster electron relaxation for smaller sized particles. This is compatible with the idea that electron relaxation is due to Auger-type energy transfer, since stronger electron–hole exchange interactions are expected for the smaller nanoparticles.

The fluorescence upconversion rises of Figure 3 are characterized by rise times (τ_1 in Table 3) in the range 700 to 1000 fs, i.e., these emission rise times are slower by about a factor of two compared to the intraband electron relaxation times of 350–550 fs. As pointed out also elsewhere,¹⁴ pump pulses near 400 nm (3.1 eV) mainly excite the $1S(e) - 3S_{3/2}(h)$ transition. Hence, in the upconversion experiment the electrons are excited predominantly directly to the lowest $1S(e)$ level and holes are prepared in highly excited hole levels. Because of the very high density of the latter, hole relaxation is initially ultrafast (< 100 fs), i.e., too fast to be detected with our setup. However, near the top edge of the hole ladder, the “emitting” and “absorbing” levels are sparsely distributed and relaxation among these levels could be relatively slow (~ 0.5 – 1 ps). Experimentally, the rise of the band-edge exciton emission is measured and since this emission originates from recombination of $1S(e)$ electrons and $1S_{3/2}(h)$ “emitting” holes, the probed rise kinetics measures the “absorbing”-to-“emitting” hole relaxation. In fact, emission is

from the $F = \pm 2$ and $F = \pm 1^L$ excitons, with energies ~ 90 meV below the energy of the $F = \pm 1^U$ state. The measured rise times of 700–1000 fs in the fluorescence upconversion experiments are typical of populating the $F = \pm 2$ and $F = \pm 1^L$ exciton states (configured from the “emitting” hole levels). In summary, the growths measured for the bleaching and fluorescence signals correspond to populating $F = \pm 1^U$ excitons and $F = \pm 2$, $\pm 1^L$ excitons, respectively. The different feeding kinetics of these excitons is caused by the different processes involved in forming these excitons: fast electron filling of the $1S(e)$ level for the $F = \pm 1^U$ and relatively slow (~ 0.7 – 1 ps) relaxation among the $1S_{3/2}(h)$ “absorbing” and “emitting” hole fine structure levels for the $F = \pm 2$, $\pm 1^L$ excitons. Equating the global Stokes shift of ~ 90 meV to the fine structure splitting between the “absorbing” and “emitting” hole levels we note that this fine structure splitting is about $3.5\hbar\omega_0$ ($\hbar\omega_0 \sim 210$ cm^{-1} is the energy of the longitudinal optical phonon). Thermal relaxation thus requires several phonons that could readily give rise to a ~ 1 ps relaxation time. Relatively slow hole filling as a final relaxation step was also reported for small CdSe quantum dots capped with a ZnS shell.¹⁴ In the latter work a hole relaxation time of about 700 fs was measured.

The fluorescence upconversion transients of Figure 3 reveal, after about 500 fs, a slight leveling off (bend) that is followed by the ~ 0.7 – 1 ps rise discussed above. So far, only feeding of the $F = \pm 1^L$ (“bright”) excitons and the less emissive $F = \pm 2$ (“dark”) excitons was mentioned, but relaxation among these close-lying states was not considered. Thermalization among these exciton states, however, will also affect the fluorescence intensity because of the different oscillator strengths of the “bright” and “dark” exciton emissions. Simulations predict a bend in the rise of the fluorescence when the rates of feeding and decay of the bright excitons are compatible. The fluorescence transients of Figure 4 thus also indicate a rapid “bright”-to-“dark” exciton relaxation, with a characteristic time that is simulated to be 230–430 fs (τ_2 in Table 3), depending on the size of the quantum dot (the smaller nanoparticles having the smaller τ_2 values). It is remarked that, since population changes of ± 2 (“dark”) and $\pm 1^L$ (“bright”) excitons are manifested in the photoluminescence intensity measurements, whereas in the bleaching experiment only population changes of the $F = \pm 1^U$ excitons are probed, it is not surprising that the bend (representative of thermal mixing of the ± 2 and $\pm 1^L$ excitons) shows up in the fluorescence rise only, and not in the bleaching recovery. In discussing the origin of the 230–430 fs component (τ_2 in Table 3), one might alternatively consider a relaxation process that involves coupling to defects at the surface.^{10,12} However, a characteristic feature of the hot-injection synthesis of the NC’s used in this work is that the annealing part optimizes surface ordering and surface reconstruction and that the concentration of surface defects is minimized.¹⁹ Also, as mentioned above, a deep trap emission, characteristic of defects or impurities,¹² could not be observed. We infer that the observed fluorescence (and also the bleaching) growths most likely are due to a mechanism “intrinsic” of the quantum dots and that electron/hole trapping to “extrinsic” surface defects is of minor importance.

Finally, we briefly discuss the multiexponential decay of the bleach and the emission signals. The decay times τ_2 (Table 1) and τ_3 (Table 3) vary from several picoseconds to several tens of picoseconds. These times are compatible with those reported in the literature.^{8,24} Auger recombination of electron–hole pairs via energy transfer to a third particle (electron or hole which is re-excited to a higher excited state) is generally assumed to be

the dominant decay process.^{8,24} In addition, coupling of the excited electron to species at the surface (adsorbed passivating layers and defects) could lead to electron trapping or extend the heat bath and hence further enhance electron relaxation.¹⁰ In our experiments, CdSe NC’s passivated with TOPO:HDA:TOP were used and thus, for our samples too, the adsorbed layers at the surface of the NC’s could contribute to the electron relaxation dynamics. In addition, at high enough laser-pump power levels, multiexciton excitation within a single quantum dot particle could take place and thus induce additional nonlinear Auger-type relaxation processes.²⁴ The laser power dependence of the transients presented in the inset of Figure 4A is indicative of contributions from multiexciton Auger relaxation. As illustrated by the inset, such processes take place on a time scale of several hundred picoseconds and thus may well account for the order of magnitude of the τ_1 values in Table 2. Note that the rise kinetics of the transients of Figure 4 is not affected by variation of the laser pump power. This implies little effect of the laser pump on the electron- and hole-level filling processes discussed above.

Acknowledgment. This research was financially supported in part by the Council for Chemical Sciences of The Netherlands Organization for Scientific Research (CW-NWO).

References and Notes

- (1) Nozik, A. J. *Annu. Rev. Phys. Chem.* **2001**, *52*, 193.
- (2) Axt, V. M.; Kuhn, T. *Rep. Prog. Phys.* **2004**, *67*, 433.
- (3) Crooker, S. A.; Barrick, T.; Hollingsworth, J. A.; Klimov, V. I. *Appl. Phys. Lett.* **2003**, *82*, 2793.
- (4) Labeau, O.; Tamarat, P.; Lounis, B. *Phys. Rev. Lett.* **2003**, *90*, 257404.
- (5) Hunsche, S.; Dekorsy, T.; Klimov, V. I.; Kurz, H. *Appl. Phys. B: Lasers Opt.* **1996**, *62*, 3.
- (6) Klimov, V. I.; McBranch, D. W. *Phys. Rev. Lett.* **1998**, *80*, 4028.
- (7) Klimov, V. I.; McBranch, D. W.; Leatherdale, C. A.; Bawendi, M. G. *Phys. Rev. B* **1999**, *60*, 13740.
- (8) Klimov, V. I. *J. Phys. Chem. B* **2000**, *104*, 6112.
- (9) Burda, C.; Link, S.; Mohamed, M.; El-Sayed, M. A. *J. Phys. Chem. B* **2001**, *105*, 12286.
- (10) Darugar, Q.; Landes, C.; Link, S.; Schill, A.; El-Sayed, M. A. *Chem. Phys. Lett.* **2003**, *373*, 284.
- (11) Guyot-Sionnest, P.; Shim, M.; Matraga, C.; Hines, M. *Phys. Rev. B* **1999**, *60*, R2181.
- (12) Underwood, D. F.; Kippeny, T.; Rosenthal, S. J. *J. Phys. Chem. B* **2001**, *105*, 436.
- (13) Efros, A. L.; Kharchenko, V. A.; Rosen, M. *Solid State Commun.* **1995**, *93*, 281.
- (14) Xu, S.; Mikhailovsky, A. A.; Hollingsworth, J. A.; Klimov, V. I. *Phys. Rev. B* **2002**, *65*, 045319.
- (15) Ekimov, A. I.; Hache, F.; Schanne-Klein, M. C.; Ricard, D.; Flytzanis, C.; Kudryavtsev, I. A.; Yazeva, T. V.; Rodina, A. V.; Efros, A. L. *J. Opt. Soc. Am. B* **1993**, *10*, 100.
- (16) Efros, A. L. *Phys. Rev. B* **1992**, *46*, 7448.
- (17) Nirmal, M.; Norris, D. J.; Kuno, M.; Bawendi, M. G.; Efros, A. L.; Rosen, M. *Phys. Rev. Lett.* **1995**, *75*, 3728.
- (18) Norris, D. J.; Sacra, A.; Murray, C. B.; Bawendi, M. G. *Phys. Rev. Lett.* **1994**, *72*, 2612.
- (19) de Mello Donegá, C.; Hickey, S. G.; Wuister, S. F.; Vanmaekelbergh, D.; Meijerink, A. *J. Phys. Chem. B* **2003**, *107*, 489.
- (20) Middelhoek, E. R.; van der Meulen, P.; Verhoeven, J. W.; Glasbeek, M. *Chem. Phys.* **1995**, *198*, 373.
- (21) Glasbeek, M.; Zhang, H. *Chem. Rev.* **2004**, *104*, 1929.
- (22) Burda, C.; Link, S.; Mohamed, M. B.; El-Sayed, M. A. *J. Chem. Phys.* **2002**, *116*, 3828.
- (23) Wang, L. W.; Califano, M.; Zunger, A.; Franceschetti, A. *Phys. Rev. Lett.* **2003**, *91*, 056404.
- (24) Klimov, V. I.; Mikhailovsky, A. A.; McBranch, D. W.; Leatherdale, C. A.; Bawendi, M. G. *Science* **2000**, *287*, 1011.